NASA Technical Memorandum 105346

A Preliminary Characterization of the Tensile and Fatigue Behavior of Tungsten-Fiber/Waspaloy-Matrix Composite

Ralph E. Corner
Sverdrup Technology, Inc.
Lewis Research Center Group
Brook Park, Ohio

and

Brad A. Lerch
National Aeronautics and Space Administration
Lewis Research Center
Cleveland, Ohio

January 1992

NASA

Trade names or manufacturers' names are used in this report for identification only. This usage does not constitute an official endorsement, either expressed or implied, by the National Aeronautics and Space Administration.

A PRELIMINARY CHARACTERIZATION OF THE TENSILE AND FATIGUE BEHAVIOR OF TUNGSTEN-FIBER/WASPALOY-MATRIX COMPOSITE

Ralph Corner
Sverdrup Technology, Inc.
Lewis Research Center Group
Brook Park, Ohio 44142

and

Brad Lerch
National Aeronautics and Space Administration
Lewis Research Center
Cleveland, Ohio 44135

E-6716

SUMMARY

A microstructural study and a preliminary characterization of the room-temperature tensile and fatigue behavior of a continuous, tungsten-fiber, Waspaloy-matrix composite was conducted. A heat treatment was chosen that would allow visibility of planar slip if it occurred during deformation, but would not allow growth of the reaction zone. Tensile and fatigue tests showed that the failed specimens contained transverse cracks in the fibers. The cracks that occurred in the tensile specimen were observed at the fracture surface and up to approximately 4.0 mm below the fracture surface. The crack spacing remained constant along the entire length of the cracked fibers. Conversely, the cracks that occurred in the fatigue specimen were only observed in the vicinity of the fracture surface. In instances where two fiber cracks occurred in the same plane, the matrix often necked between the two cracked fibers. Large groups of slip bands were generated in the matrix near the fiber cracks. Slip bands in the matrix of the tensile specimen were also observed in areas where there were no fiber cracks, at distances greater than 4 mm from the fracture surface. This suggests that the matrix plastically flows before fiber cracking occurs.

INTRODUCTION

Tungsten-reinforced Waspaloy (W/Waspaloy) has potential use in high-temperature, severe-environments, such as turbine blades in the space shuttle main engine. Accurate modeling of this material is a prerequisite to introducing it into service. To this end, the correct deformation and damage behavior must be thoroughly understood. Of particular interest is the deformation behavior of the matrix. It has been shown in silicon carbide (SiC) reinforced Ti-15-3 (ref. 1) that the matrix deforms plastically during tensile loading. The matrix flowed plastically, as evidenced by slip bands in the matrix, before the SiC fibers cracked. To investigate whether the behavior of W/Waspaloy would be similar, the composite was given a pretest heat treatment to produce an underaged precipitate state. In this state, any matrix plasticity should

manifest itself in the form of distinct slip bands (refs. 2 and 3), and these slip bands should be easily observed upon metallographic investigations. During metallographic studies on this material, other forms of damage would also become evident.

This work was a preliminary characterization of tensile and fatigue damage. A limited amount of material was available and, as such, the study is by no means exhaustive. However, some familiarity with microstructure and general mechanical behavior of this composite was gained, and ideas are presented for future work when additional material becomes available.

EXPERIMENTAL PROCEDURE

The W/Waspaloy composite material was fabricated using an arc spray process. The composite plate was reinforced with four plys of unidirectional ($[0]_4$), Phillips Elmet (ST-300), tungsten (W-1.5%-ThO_2) fibers of 190 μm diameter. The plate was then hot isostatic pressed (HIPed) into a 1.37-mm-thick plate. The fiber volume fraction was nominally 40 percent. The Waspaloy matrix nominal composition was measured using an atomic emission spectroscopy process and yielded: 61Ni, 17Cr, 13Co, 4Mo, 2Al, 2Ti, 0.04C, 0.007B, 0.003Zr in weight percent.

In order to investigate aging of the Waspaloy matrix within the composite, coupons (1 cm^2) were exposed to various heat treatments as given in table I. After the heat treatments, the coupons were then sectioned, prepared metallographically, and etched with a solution of 15 ml HCl (37 percent), 10 ml HNO_3 (70 percent), and 10 ml acetic acid. The samples were examined using an optical microscope to determine what changes, if any, occurred in the microstructure due to the heat treatments. Heat treatment effects were also determined using hardness tests in which approximately 10 Vickers hardness measurements were made on each sample with a 200-gram load. Each hardness indentation was placed in the center of an interior matrix grain and away from the fibers.

Two tensile and one low-cycle-fatigue (LCF) specimens were cut from the composite plate such that the fiber axis was parallel to the loading direction. The specimen geometry was rectangular having dimensions of 76 by 13 mm. The specimens were heat treated as follows:

(1) Solution at 1200 °C for 2 hr
(2) Water quench to room temperature
(3) Age at 730 °C for 6 hr
(4) Water quench to room temperature

The specimens were tested at room temperature using a closed-loop servohydraulic testing machine. A stainless-steel tab, 25 mm long by 13 mm wide by 2.5 mm thick, was placed on each end and on each side of the specimen using a cyanoacrylate adhesive. This was done to accommodate the inside dimensions of the grip and to

enable the proper grip pressure to be applied. Because the specimen was so short, an extensometer could not be used; hence, strain measurements were not taken. The tensile specimens were tested in stroke control at a constant crosshead displacement rate of 2.4×10^{-3} mm/sec. One specimen was tested to failure, and the other was interrupted before its ultimate tensile strength was reached. The LCF specimen was tested in load control at 0.17 Hz. A triangular waveform was used, ramping between stress amplitudes of 30 and 700 MPa.

After testing, the specimens were sectioned and scanning electron microscopy (SEM) was performed to study the fracture surfaces of the specimens. Thereafter, the specimens were polished and etched using the etchant mentioned previously and then analyzed metallographically for damage and microstructural changes. The polished specimens were then sputter coated with palladium and examined using the SEM for better resolution.

RESULTS AND DISCUSSION

As-Received Material Characterization

The as-received composite configuration is shown in figure 1. The fibers are arranged in a square array with an average edge length of 0.25 mm between fiber centers. The matrix appeared relatively free of grain boundary particles; therefore, it was necessary to have the sample metallographically overetched to reveal the grain structure. This resulted in blackened areas surrounding some of the fibers (fig. 1) as well as uneven etching of the grain boundaries. Metallographic and SEM investigations revealed that a 1-1.5-μm-thick reaction zone had developed between the fiber and the matrix (fig. 2). Using the SEM and energy dispersive spectroscopy (EDS), it was concluded that the composition of the reaction zone was primarily composed of W, Cr, and Ni. In addition, the as-received material contained some split fibers (figs. 1 and 3). These splits contained a reaction product (fig. 3) primarily consisting of Al, Ti, W, and Cr. As will be shown in later figures, these cracks opened during testing and were especially evident after fatigue loading.

Heat Treatments

Various heat treatments (table I) were performed on composite coupons. The heat treatments consisted of a solution treatment and an aging treatment. The solution treatment was varied to study its effect on grain size and reaction zone size with the goal of minimizing the growth of each. The aging conditions were chosen such that small precipitates would form which would be easily sheared by dislocations during straining, thus creating well-defined and easily observed planar slip. The conditions were based on a previous study performed on monolithic Waspaloy (ref. 2).

The heat treatment study showed that there were no obvious grain size differences in the matrix observed for the heat treatments used in this study. There was a large

distribution of grain sizes within the matrix in each sample, and this prevented a meaningful grain size number from being determined. An example of the matrix grain structure after a heat treatment of 1200 °C for 2 hr, water quench, 730 °C for 6 hr, and a water quench can be seen in figure 4. Similarly, the size of the reaction zone did not vary with heat treatment.

The relationships between matrix hardness and heat treatment (table I) reveal that the aging treatment produced a slightly harder material than the solution (1300 °C for 7 hr) treatment. This was expected since aging at 730 °C for 6 hr should have precipitated underaged γ' particles in the matrix (ref. 2). The resulting small precipitates were easily sheared by dislocations during plastic deformation, thereby producing distinct slip bands. Such slip bands are evident emanating from a hardness indentation in figure 5.

Tensile Tests

As seen in figure 6, the stress versus stroke curve remains approximately linear to 230 MPa. Thereafter, nonlinear behavior is observed until a maximum stress of 825 MPa is reached, and failure occurred. The specimen fractured in the grips most likely due to the size of the specimen. Note that the specimen size was limited by material availability and is not the size generally used for tensile and fatigue tests. The ultimate tensile strength (UTS) of 825 MPa was similar to the UTS measured in a previous study on W/Waspaloy (ref. 4).

From a rule of mixtures (ROM) calculation, the UTS of the composite was calculated to be

$$UTS_{comp} = (UTS_{fiber} \times V_{fiber}) + UTS_{matrix} \times (1 - V_{fiber}) = 1490 \text{ MPa}$$

where

$$V_{fiber} = 40 \text{ percent}$$

$$UTS_{fiber} = 2520 \text{ MPa}$$

(from unpublished data obtained by P. Brindley of Lewis) and

$$UTS_{matrix} = 770 \text{ MPa}$$

at 1 percent strain (ref. 2). That value is substantially higher than the observed UTS indicates that the composite did not reach its full strength potential possibly because of to the fabrication process.

SEM fractography of the failed tensile specimen (fig. 7), revealed a flat fracture surface. There was no evidence of fiber pull-out, indicating a good fiber/matrix interfacial bond. The matrix broke in a ductile fashion as indicated by the necking

surrounding the fibers and by the microvoid coalescence (not shown in fig. 7). Figure 8 shows a longitudinal cross section of the second ply including the fracture surface. No secondary cracks were observed in the matrix; however, the fibers contained many transverse cracks. Three fibers were randomly selected to measure the lengths of the segments between fiber cracks as a function of distance from the fracture surface. The method for which the measurements were taken is shown in figure 8. The average measurements, taken on three fibers, show that the segment length was 0.15±0.10 mm and was constant throughout the length of the cracked fiber. The fiber cracking ceased at a distance of 4 mm from the fracture surface.

The critical fiber length L_c at which the fiber segment carries a stress equal to its tensile strength is given in reference 5 as

$$L_c = \sigma_f D_f / 2\tau$$

where σ_f is the fiber strength (2520 MPa), D_f is its diameter (190 μm), and τ is the shear strength of the matrix (595 MPa). The critical fiber length was calculated to be 0.4 mm, which is larger than the average measured segment length of 0.15 mm. This, again, indicates that the composite is not realizing its full potential. One possible explanation for the small fiber segment lengths and the low experimental UTS compared with the ROM calculation could lie with a weak fiber. The consolidation process may have degraded the fiber from its standalone strength of 2520 MPa. Additionally, it is not known what effect the split fibers have on the critical fiber length and the resulting composite strength.

Slip bands occurred extensively in areas of the matrix where the fibers were cracked (i.e., along the 4-mm length below the fracture surface). As seen in the areas where two adjacent fibers cracked in the same plane, matrix necking occurred (fig. 9(a)). The necked area contained slip bands which produced an X-pattern. Throughout these areas, the reaction zone separated from the fiber, but adhered to the matrix. The reaction zone contained many transverse cracks in these debonded areas.

In the areas where the fibers cracked, but where there was no matrix necking, slip bands often occurred in the matrix. The slip bands in the matrix connected the fiber cracks on either side of the matrix producing a V-pattern (fig. 9(b)). Slip bands were also observed in areas where the fibers were not cracked, that is, at distances greater than 4 mm below the fracture surface (fig. 10), which suggests that the matrix can flow plastically before fiber cracking occurs.

The second tensile test was interrupted before the UTS at a stress of 645 MPa (i.e., in the nonlinear region of the tensile curve, fig. 6) and examined to determine what damage occurred. The entire specimen was examined metallographically. There was no sign of damage or matrix slip bands, nor was there an increase in matrix microhardness (table II), which would indicate work hardening of the matrix due to plasticity. It is therefore unclear what causes the nonlinearity in the tensile curve. Based on the failed sample, in which slip bands were observed in the matrix in areas where the fibers were

still intact, it is believed that matrix plasticity occurs first followed by fiber cracking. However, more specimens will have to be tested to confirm this.

Fatigue Test

The LCF specimen was tested at a stress range of 670 MPa. This yielded a life of 32 352 cycles. The specimen fractured just outside of the bottom grips, again, probably due to the size of the specimen. Due to the stress concentration in the grip area, the actual fatigue life may be longer than the one reported here. The stress-stroke response for the first two cycles is plotted in figure 11. A large, nonrecoverable strain is observed in the first cycle. The second cycle is primarily linear. Minimal strain ratcheting was observed throughout the test. Similar to the tensile specimen, the SEM fractography of the LCF specimen (fig. 12) shows no evidence of fiber pull-out and also depicts the matrix as having a ductile fracture, as evidenced by the necking around the fibers. Figure 12 shows that the fiber splits have opened and are much more visible than in the as-received materials (fig. 1).

As seen in the longitudinal cross section (fig. 13), the fibers were cracked, but only close (0.5 mm) to the fracture surface. This is significantly smaller than the distance over which fibers were cracked for the tensile specimen (4 mm) and indicates the extreme localization of damage that occurs during fatigue. The average segment length was measured to be 0.20 ± 0.12 mm, which is not too unlike the segment length observed in the tensile specimen. The slip band occurrences and formations were relatively the same as in the tensile specimen; however, there were fewer occurrences since the number of transverse fiber cracks were fewer. As seen in table II, the hardness of the fatigue sample was similar to the hardness of the as-received coupon, again, indicating that work hardening of the matrix was minimal.

The localization of damage near the fracture surface suggests that a crack initiates at a single location (perhaps a surface defect) and propagates through the specimen. The stress range does not appear high enough to initiate damage throughout the specimen length. The actual progression of fatigue damage still needs to be verified when more specimens become available.

SUMMARY OF RESULTS

A microstructural study was performed on a tungsten-fiber-reinforced Waspaloy composite. Optical and scanning electron microscopy, x-ray spectroscopy, atomic emission spectroscopy, and hardness measurements were used to characterize the initial microstructure. Two tensile tests and one fatigue test were performed on the specimens and examined for damage. A summary of the findings are listed below.

1. The W/Waspaloy fiber distribution within the matrix formed a square array. The average fiber center-to-center distances was 0.25 mm. The average fiber volume fraction was 40 percent.

2. A reaction zone measuring 1 to 1.5 μm thick and consisting of W, Cr, and Ni developed between the fiber and the matrix.

3. The as-received material contained split fibers.

4. Transverse fiber cracks were observed in failed tensile and fatigue samples.

5. The transverse fiber cracks in the tensile specimen were restricted to an area from the fracture surface to 4 mm below the fracture surface. The length of fiber segments between fiber cracks was constant over the 4-mm length.

6. Slip bands were observed in the matrix near the cracked fibers.

7. Fatigue damage was localized near the fracture surface.

The observations reported here indicate that a better understanding of damage development will be necessary before constitutive or life-prediction modeling can commence. To this end, more interrupted tests will be needed. Since matrix plasticity is believed to be a major contributor to deformation, this work concentrated on the observation of slip bands. By creating a precipitate, size through heat treatment, that was conducive to planar slip, some slip bands could be observed in failed samples. However, more extensive plasticity may be occurring during deformation and was not observed using only optical microscopy. Future studies should employ transmission electron microscopy to determine the point at which matrix flow begins. Failure to do this could lead to false conclusions regarding the constitutive behavior.

REFERENCES

1. Lerch, B.A.: Matrix Plasticity in SiC/Ti-15-3 Composite. NASA TM-103760, 1991.

2. Lerch, B.A.: Microstructural Effects on the Room and Elevated Temperature Low Cycle Fatigue Behavior of Waspaloy. NASA CR-165497, 1982.

3. Diederich, D.; Lerch, B.A.; and Antolovich, S.D.: Observations of Low Cycle Fatigue and Fatigue Crack Propagation Substructures in Waspaloy. 8th Inter-American Conference on Materials Technology, Organization of American States, Washington, D.C., 1985, pp. 7.1-7.6.

4. Yuen, J.L.: Screening Evaluation of Candidate Fiber-Reinforced Superalloys for Space Shuttle Main Engine Turbopump Blade Application, Part I. NASA CR-175085, 1986.

5. Kelly, A.; and Tyson, W.R.: Fiber Strengthened Materials. High Strength Materials, V.F. Zackay, ed., John Wiley and Sons, 1965, pp. 578-602.

TABLE I.—COUPON HEAT TREATMENT CONDITIONS

Heat treatment conditions, °C/hr (a)	Vickers hardness
As-received	386.6±15.3
1300/7	377.0±29.7
1100/2+WQ+730/6+WQ	413.0±23.6
1200/2+WQ+730/6+WQ	401.8±23.6
1200/6+WQ+730/6+WQ	398.9±21.3

[a]WQ denotes water quench.

TABLE II.—SPECIMEN HEAT TREATMENT CONDITIONS

Specimen	Heat treatment conditions, °C/hr (a)	Vickers hardness	Fiber volume fraction, percent
Failed tensile	1200/2+WQ+730/6+WQ	388.7±20.3	41
Interrupted tensile	1200/2+WQ+730/6+WQ	389.7±21.7	33
Fatigue	1200/2+WQ+730/6+WQ	376.7±19.7	35

[a]WQ denotes water quench.

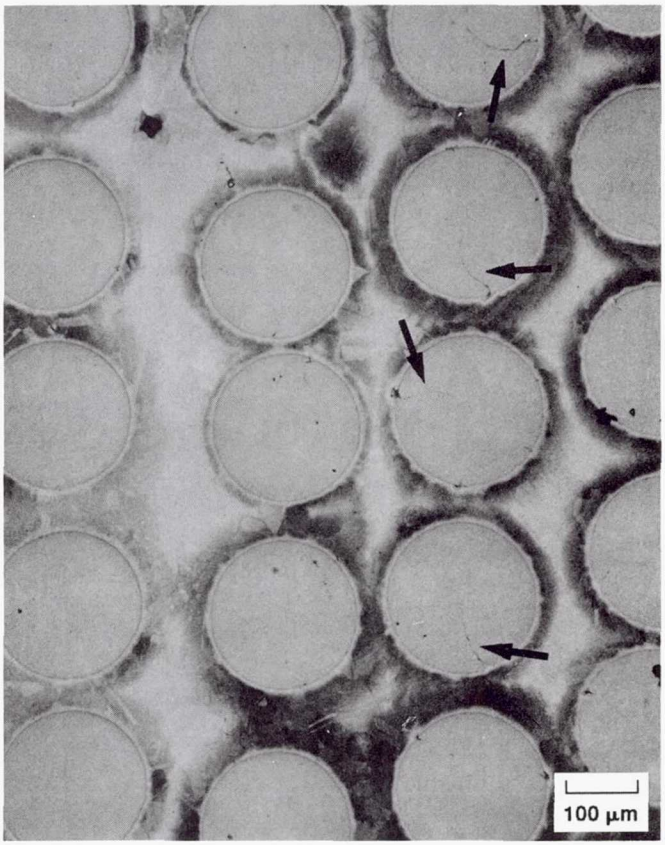

Figure 1.—As-received microstructure of W/Waspaloy (etched). Arrows indicate fiber splits.

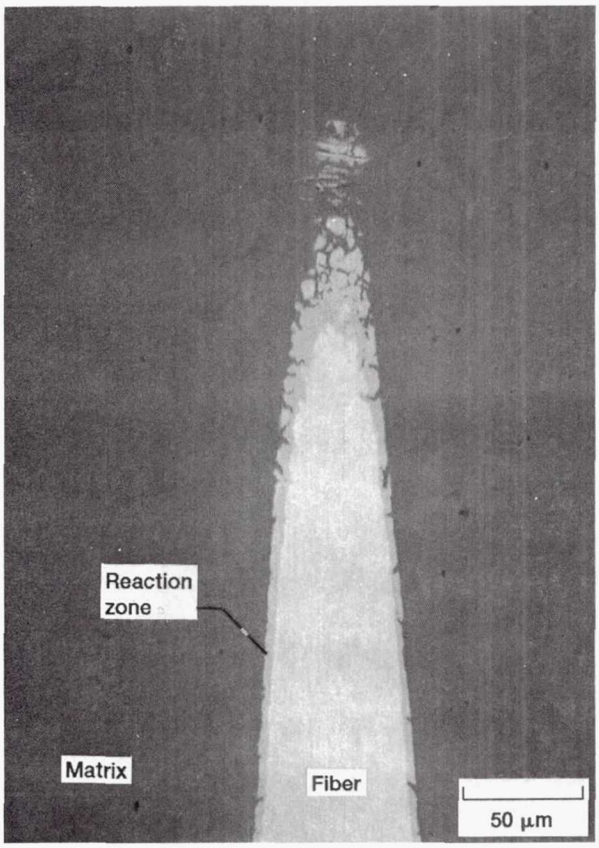

Figure 2.—Metallographic cross-section of reaction zone developed between the fiber and the matrix. Scanning (backscatter) electron micrograph.

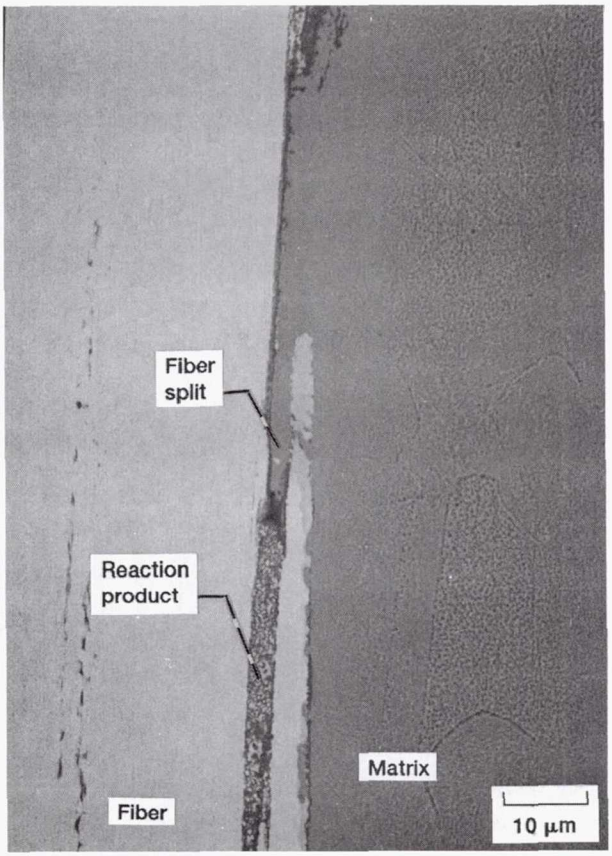

Figure 3.—Scanning (backscatter) electron micrograph of a split fiber which is filled with a reaction product.

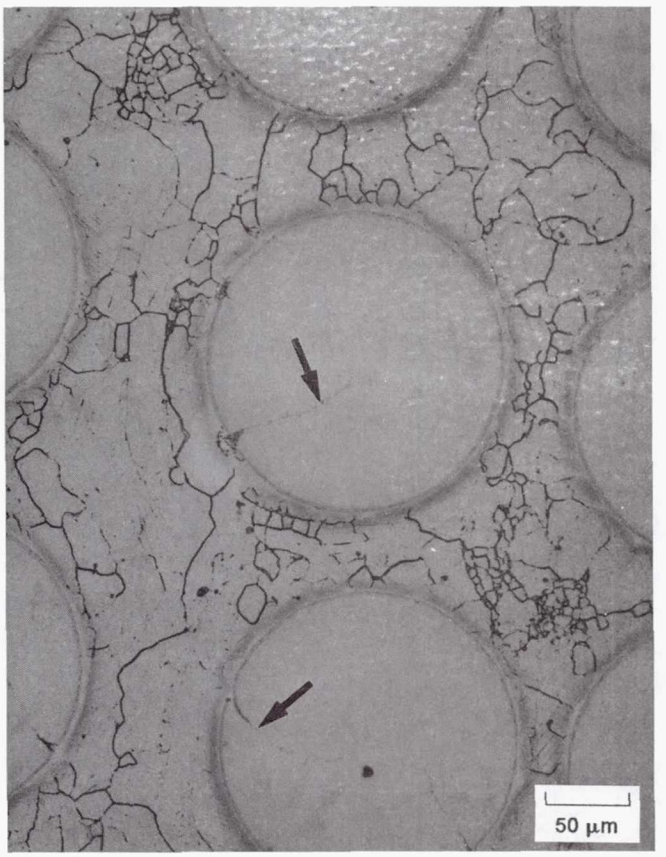

Figure 4.—Typical grain size distribution of an aged W/Waspaloy matrix. Arrows indicate split fibers. Heat treatment, 1200 °C for 2 hr + WQ + 730 °C for 6 hr + WQ.

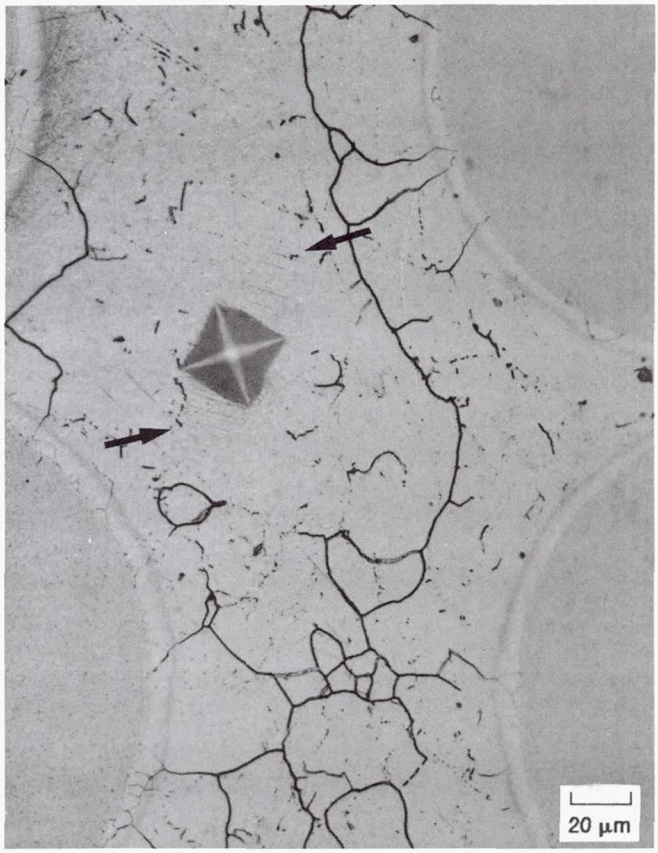

Figure 5.—Slip bands (arrows) occurring in the matrix from Vickers hardness indentation.

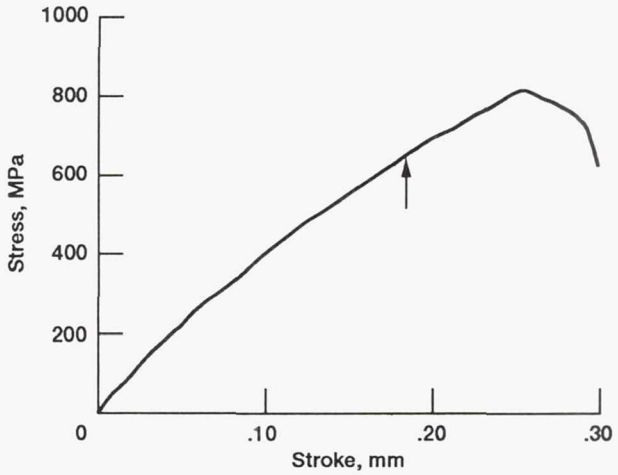

Figure 6.—Room-temperature tensile curves. Arrow indicates where a second test was interrupted before failure. The curve for the interrupted test overlayed the test-to-failure curve.

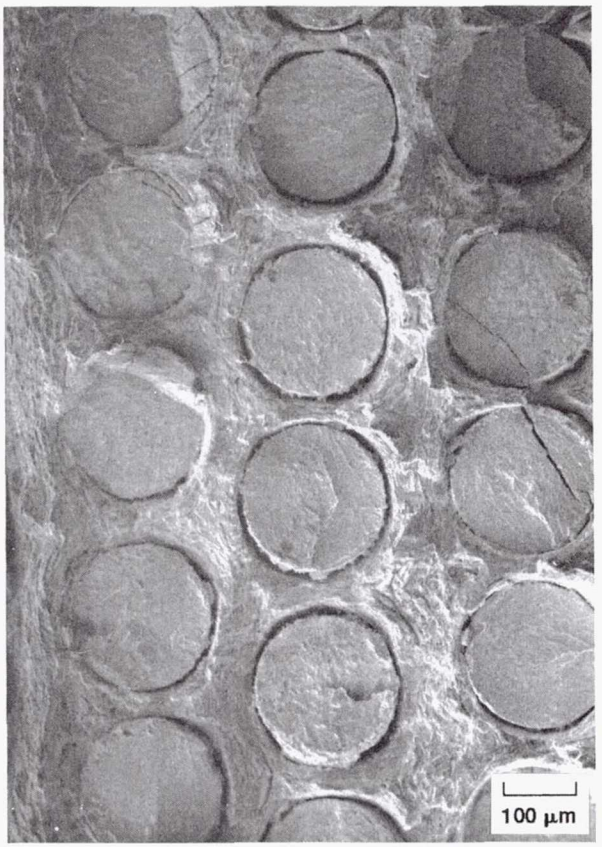

Figure 7.—SEM micrograph showing the fracture surface of tensile specimen.

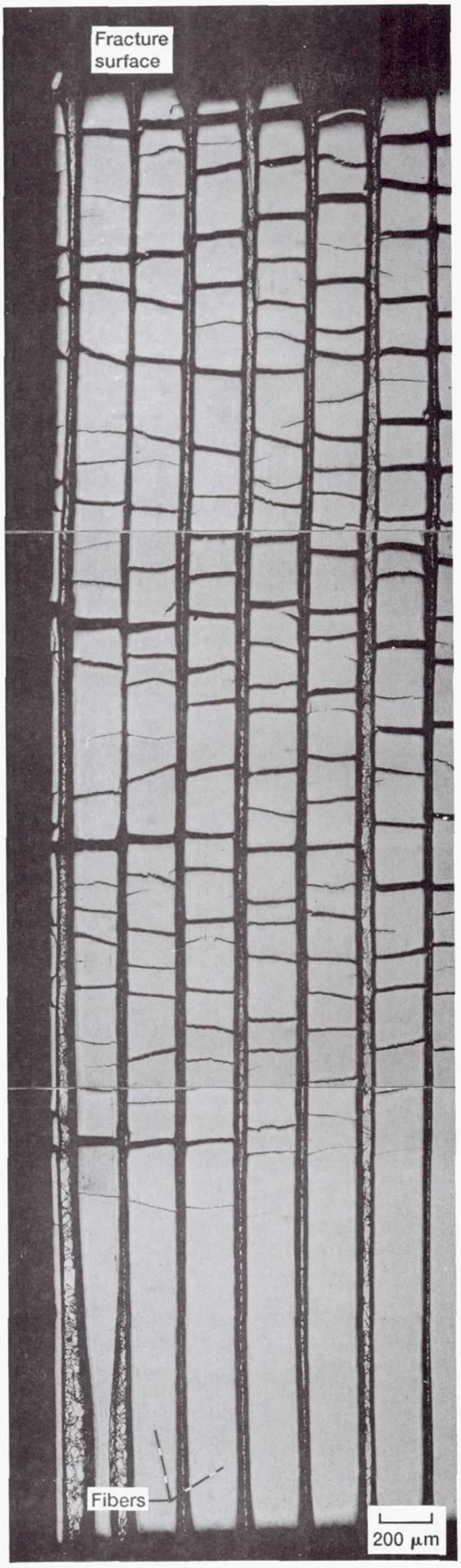

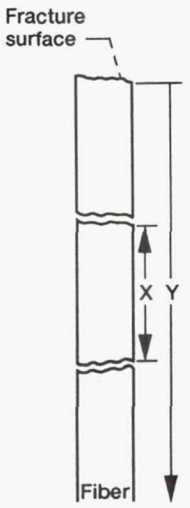

X = Fiber segment length (mm) between cracks

Y = Cumulative length (mm) of fiber segments beginning at the fracture surface

Figure 8.—Longitudinal cross-section of the fracture surface showing the transverse fiber cracks and fiber segment length that occurred in the tensile specimen.

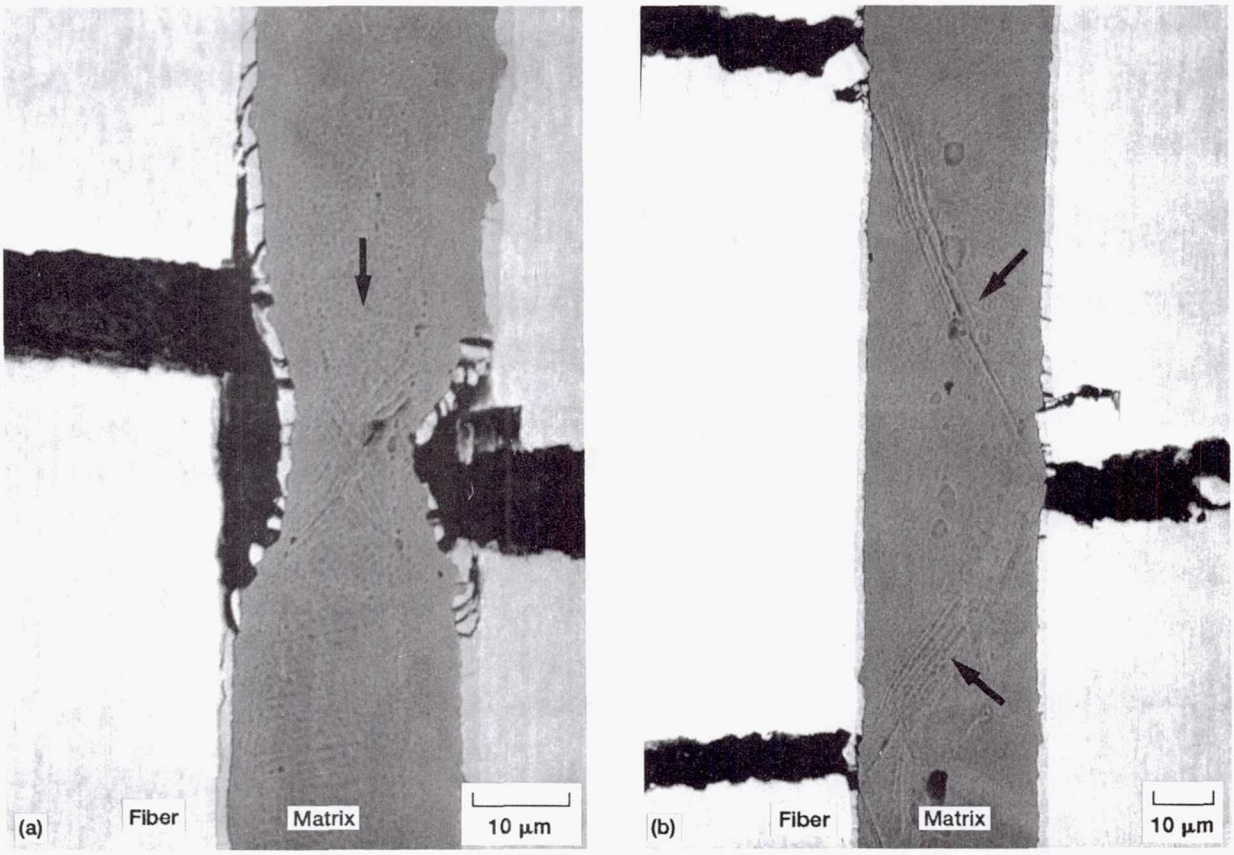

Figure 9.—SEM (BSE) micrographs of failed tensile specimen. Matrix necking occurred in areas where fibers cracked in the same plane. Slip bands (arrows) producing an X pattern also developed (a). Slip bands (arrows) in the pattern of a V were formed in areas where the cracks in adjacent fibers alternated.

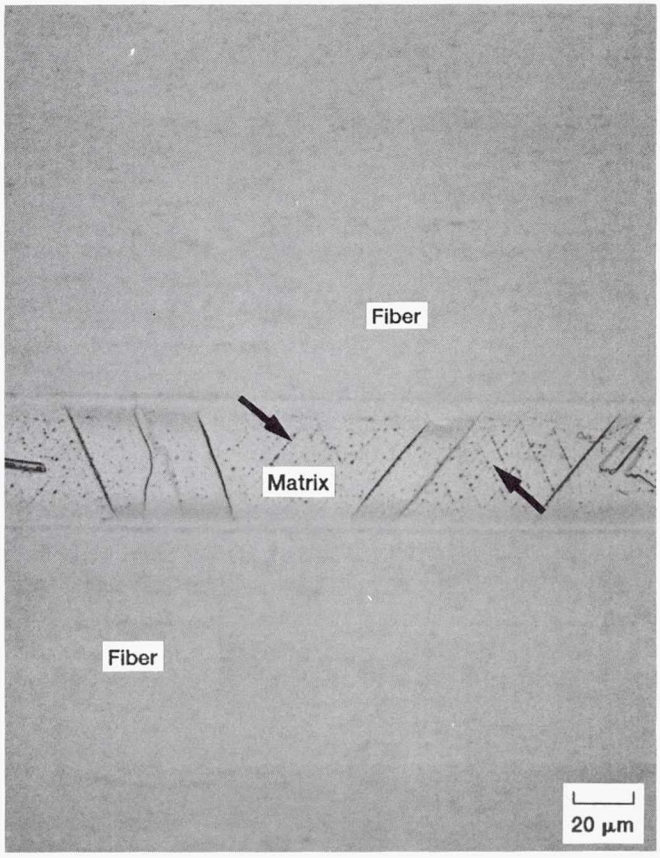

Figure 10.—Slip bands (arrows) in the matrix, away from the fracture surface. Optical micrograph.

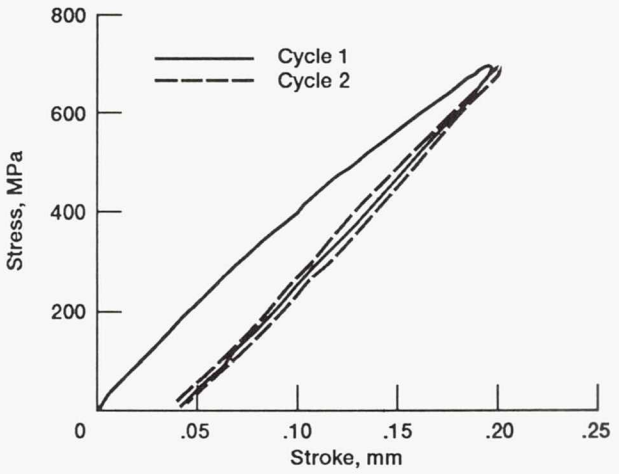

Figure 11.—Room-temperature cyclic stress-stroke curves of LCF specimen.

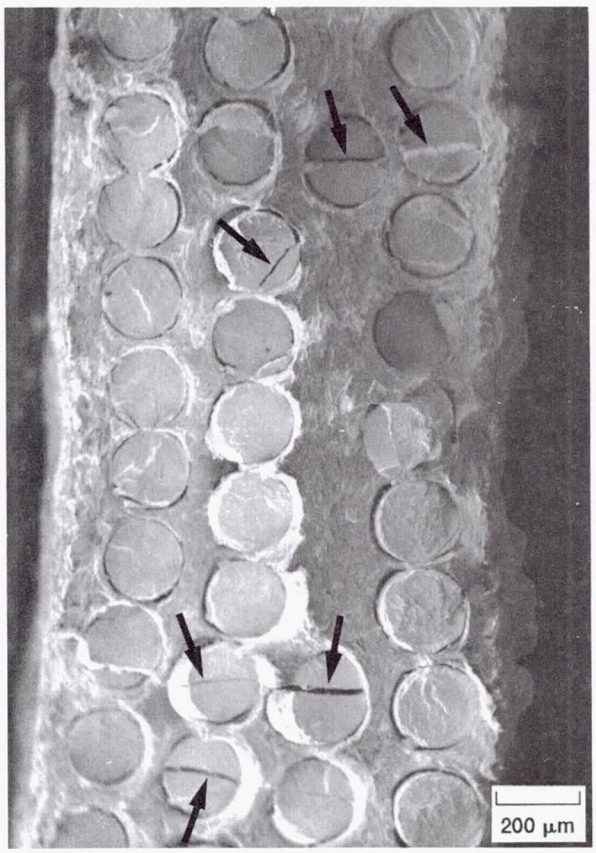

Figure 12.—SEM micrograph showing fracture surface of LCF specimen. Notice missing fibers in the third ply. Arrows indicate fiber splits.

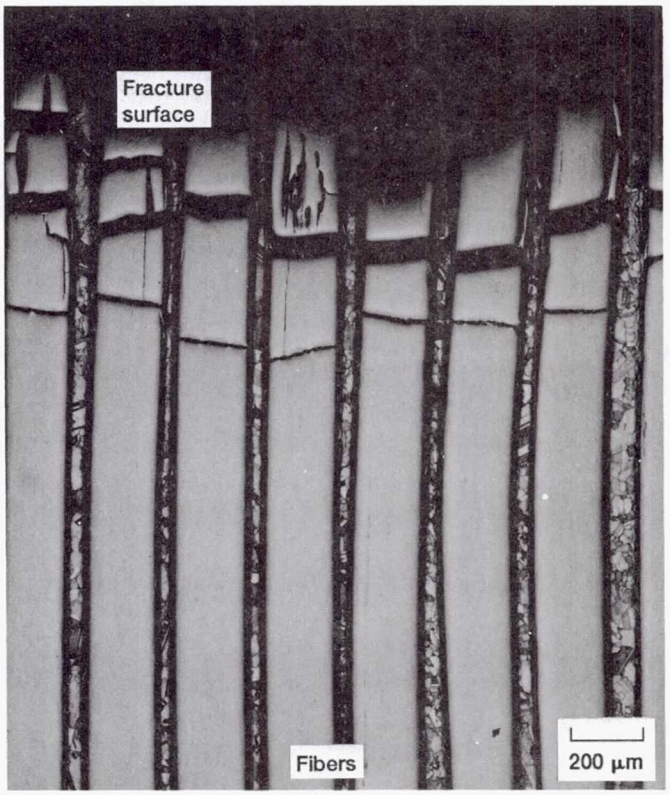

Figure 13.—Longitudinal cross section of the fracture surface showing transverse fiber cracks that occurred in LCF specimen and resulting fiber segment lenghts.

REPORT DOCUMENTATION PAGE

Form Approved
OMB No. 0704-0188

1. AGENCY USE ONLY (*Leave blank*)	2. REPORT DATE	3. REPORT TYPE AND DATES COVERED
	February 1992	Technical Memorandum

4. TITLE AND SUBTITLE

A Preliminary Characterization of the Tensile and Fatigue Behavior of Tungsten-Fiber/Waspaloy-Matrix Composite

5. FUNDING NUMBERS

WU-510-01-50

6. AUTHOR(S)

Ralph E. Corner and Brad A. Lerch

7. PERFORMING ORGANIZATION NAME(S) AND ADDRESS(ES)

National Aeronautics and Space Administration
Lewis Research Center
Cleveland, Ohio 44135-3191

8. PERFORMING ORGANIZATION REPORT NUMBER

E-6716

9. SPONSORING/MONITORING AGENCY NAMES(S) AND ADDRESS(ES)

National Aeronautics and Space Administration
Washington, D.C. 20546-0001

10. SPONSORING/MONITORING AGENCY REPORT NUMBER

NASA TM-105346

11. SUPPLEMENTARY NOTES

Ralph E. Corner, Sverdrup Technology, Inc., Lewis Research Center Group, 2001 Aerospace Parkway, Brook Park, Ohio 44142; Brad A. Lerch, NASA Lewis Research Center. Responsible person, Brad A. Lerch, (216) 433-5522.

12a. DISTRIBUTION/AVAILABILITY STATEMENT

Unclassified - Unlimited
Subject Category 34

12b. DISTRIBUTION CODE

13. ABSTRACT *(Maximum 200 words)*

A microstructural study and a preliminary characterization of the room-temperature tensile and fatigue behavior of a continuous, tungsten-fiber Waspaloy-matrix composite was conducted. A heat treatment was chosen that would allow visibility of planar slip if it occurred during deformation but would not allow growth of the reaction zone. Tensile and fatigue tests showed that the failed specimens contained transverse cracks in the fibers. The cracks that occurred in the tensile specimen were observed at the fracture surface and up to approximately 4.0 mm below the fracture surface. The crack spacing remained constant along the entire length of the cracked fibers. Conversely, the cracks that occurred in the fatigue specimen were only observed in the vicinity of the fracture surface. In instances where two fiber cracks occurred in the same plane, the matrix often necked between the two cracked fibers. Large groups of slip bands were generated in the matrix near the fiber cracks. Slip bands in the matrix of the tensile specimen were also observed in areas where there were no fiber cracks, at distances greater than 4 mm from the fracture surface. This suggests that the matrix plastically flows before fiber cracking occurs.

14. SUBJECT TERMS

Composite material; Metal matrix composite; Heat treatment; Microstructure; Tensile deformation

15. NUMBER OF PAGES

18

16. PRICE CODE

A03

17. SECURITY CLASSIFICATION OF REPORT	18. SECURITY CLASSIFICATION OF THIS PAGE	19. SECURITY CLASSIFICATION OF ABSTRACT	20. LIMITATION OF ABSTRACT
Unclassified	Unclassified	Unclassified	